



UvA-DARE (Digital Academic Repository)

Dynamics of water interacting with biomolecules

Groot, C.C.M.

Publication date

2017

Document Version

Other version

License

Other

[Link to publication](#)

Citation for published version (APA):

Groot, C. C. M. (2017). *Dynamics of water interacting with biomolecules*. [Thesis, externally prepared, Universiteit van Amsterdam].

General rights

It is not permitted to download or to forward/distribute the text or part of it without the consent of the author(s) and/or copyright holder(s), other than for strictly personal, individual use, unless the work is under an open content license (like Creative Commons).

Disclaimer/Complaints regulations

If you believe that digital publication of certain material infringes any of your rights or (privacy) interests, please let the Library know, stating your reasons. In case of a legitimate complaint, the Library will make the material inaccessible and/or remove it from the website. Please Ask the Library: <https://uba.uva.nl/en/contact>, or a letter to: Library of the University of Amsterdam, Secretariat, Singel 425, 1012 WP Amsterdam, The Netherlands. You will be contacted as soon as possible.

5 WATER DYNAMICS IN AQUEOUS SUGAR SOLUTIONS

Sugars are an important class of biological molecules. In living organisms, they fulfill a wide range of functions, serving for example as an energy source or signaling group (when part of a glycoprotein or glycolipid), or acting as a stabilizing osmolyte of proteins under environmental stress conditions^{78,79}. This latter property is still not fully understood, though it has been hypothesized that sugars stabilize proteins against unfolding indirectly, via the water solvent. In this chapter we study the effect of the sugars glucose, trehalose and sorbitol on the reorientation dynamics of water molecules. We find that at all sugar concentrations the water dynamics can be described by a single reorientation time constant. With increasing carbohydrate concentration, the water reorientation time constant increases from 2.5 picoseconds to a value of about 15 picoseconds. The slowing down of the water dynamics is strongest for trehalose, followed by glucose and sorbitol. Compared to other small amphiphilic solutes, the influence of sugars on the dynamics of water is relatively long-ranged, and involves collective structural effects. These results are in line with an indirect protection mechanism of sugars via the water solvent.

5.1 INTRODUCTION

Sugars are known to stabilize proteins against unfolding under extremely cold and dry conditions. Even though this latter property is widely used in industry and in biochemistry labs, the exact mechanism by which sugars stabilize proteins against unfolding is still not fully understood^{78–80}.

Since sugars are preferentially excluded from protein surfaces^{78,79}, it has been hypothesized that they protect proteins indirectly by modifying the properties of the water solvent. For this reason, people have extensively investigated the properties of water in solutions of sugars, using a wide range of techniques. With Raman spectroscopy^{81–83}, neutron scattering⁸³, neutron diffraction^{84–86} and THz absorption experiments^{87,88}, it was found that the water structure around sugars is changed in comparison to the structure of neat water. However, the observed structural changes tend to be quite small⁸⁶. A more pronounced effect is found with techniques that probe the dynamics of the water molecules. Dielectric relaxation⁸⁹, NMR⁹⁰, time-resolved fluorescence⁹¹ and dynamic light scattering^{92,93} studies all show that the dynamics of water slows down significantly near sugar molecules. A similar slowing down effect is seen with molecular dynamics simulations^{81,94–96}. However, the different studies do not agree on the magnitude and the spatial extent of the effects of sugar molecules on the dynamics of water. For trehalose, for example, which is the sugar with the highest degree of bioprotectability, different techniques give different results. With NMR measurements of the spin relaxation rate of water ¹⁷O in dilute trehalose solutions, a modest retardation factor of 1.6 was found, assuming that the hydration shell consists of 47 water molecules⁹⁰. In dynamic light scattering measurements⁹², a much larger retardation factor of 5 to 6 was found, for a hydration shell consisting of 25 water molecules. Finally, time-dependent fluorescence Stokes shift measurements of a small THz probe covalently attached to trehalose⁹¹, indicate that trehalose retards the dynamics of more than 150 surrounding water molecules by a factor of ~ 2 .

In this chapter we investigate the effect of glucose, trehalose and sorbitol on water reorientation dynamics. To this end, we use polarization-resolved pump-probe spectroscopy, which directly measures the reorientation dynamics of both water and solute. The selected sugars are all commonly used as stabilizing osmolyte, and have some interesting properties of their own: glucose is the main monosaccharide unit and energy source in biological systems, trehalose is known to be the most bioprotective sugar⁸⁰, and sorbitol is a linear form of glucose, and the comparison with glucose allows us to study the effect of the sugar conformation on the water reorientation dynamics.

5.2 EXPERIMENTAL

SPECTROSCOPY The measurements described in this chapter are performed with the single-color setup described in section 3.2. The pump and probe pulses are centered around 2500 cm^{-1} , in resonance with the OD stretch vibration.

To probe the dynamics of the rise in sample temperature, the dual-color setup described in section 3.3 is used as well, with a modified pump generation scheme: a BBO-based OPA (TOPAS, LightConversion) creates signal and idler pulses of $1.33 \mu\text{m}$ and $2 \mu\text{m}$ respectively. The idler pulses are subsequently doubled in a 4 mm BBO crystal and mixed with 800 nm light in a 10 mm lithiumniobate crystal, to generate $24 \mu\text{J}$ pump pulses centered at 2500 cm^{-1} with a bandwidth of 100 cm^{-1} (FWHM). The crystals are chosen to be relatively thick, to generate a pump spectrum that has the same bandwidth as the single-color setup. The probe pulses of the dual-color setup are centered at 2950 cm^{-1} , in resonance with the low-frequency tail of the OH stretch vibration.

SAMPLE PREPARATION Glucose, trehalose and sorbitol were purchased from Sigma-Aldrich (purity $>98\%$) and mixed with H_2O and D_2O , such that the percentage of deuterated hydroxyl groups in the sample was always 4%. After mixing, we stirred and heated the solutions to about 50°C to promote dissolution. Upon cooling back to room temperature, the carbohydrates stayed well dissolved.

5.3 RESULTS

5.3.1 LINEAR SPECTRA

Figure 5.1 presents linear spectra of solutions of glucose in isotopically diluted water. The spectra show a broad absorption band centered at 2500 cm^{-1} due to the OD stretch vibrations of water and glucose. With increasing glucose concentration, the center frequency and spectral shape show little change. The absorption around 2500 cm^{-1} slightly decreases, due to the decrease of the concentration of OD oscillators, and the absorption at frequencies above 2600 cm^{-1} increases, due to the absorption of the CH stretch vibrations of glucose. The same trends are observed for solutions of trehalose and sorbitol in isotopically diluted water.

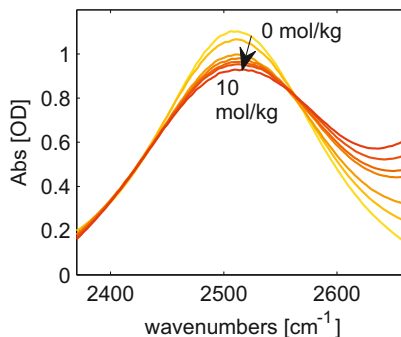


FIGURE 5.1. Linear spectra of aqueous glucose solutions (0, 1, 2, 3, 5, 7, 10 mol/kg), with 4%D:H. The spectra are corrected for H_2O background.

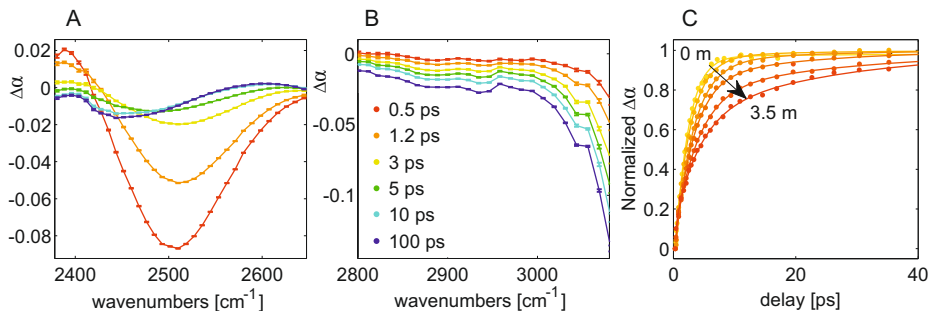


FIGURE 5.2. Isotropic absorption change for solutions of trehalose in water at different picosecond delay times after excitation with a 2500 cm^{-1} pump pulse. (A) Absorption change between 2400 and 2600 cm^{-1} (OD stretch vibration) for 3.5 molal trehalose. (B) Absorption change between 2800 and 3100 cm^{-1} (tail of OH stretch vibration, heating signal) for 3.5 molal trehalose. (C) Absorption change between 2800 and 3100 cm^{-1} , normalized at 100 picoseconds, for different concentrations of trehalose (0 , 0.5 , 1 , 1.5 , 2.5 and 3.5 molal). The lines represent empirical triple-exponential fits.

5.3.2 ISOTROPIC AND ANISOTROPIC SIGNALS

In figure 5.2 we present isotropic transient absorption signals measured for solutions of trehalose after exciting the sample with a pump pulse at 2500 cm^{-1} . Figure 5.2A presents the isotropic absorption signal between 2400 and 2600 cm^{-1} for a solution of 3.5 molal trehalose. At early delay times, we observe a bleach at the fundamental transition of the OD stretch vibration around 2500 cm^{-1} , and an induced absorption at frequencies below 2420 cm^{-1} . At later delay times, these signals have decayed and the transient spectral response is formed by a thermal difference spectrum. Figure 5.2B presents the isotropic absorption signal between 2800 and 3100 cm^{-1} for the same solution. The bleaching signal (negative absorption change) slowly rises with increasing delay time. This signal is due to the shift and decrease in cross section of the OH stretch vibrations with temperature, and directly represents the rise in sample temperature. The dynamics of the heat signal between 2800 and 3100 cm^{-1} (normalized at 100 picoseconds) for different concentrations of trehalose are shown in figure 5.2C. With increasing concentration of trehalose, the heat dynamics slow down considerably. For solutions of glucose and sorbitol we observe a similar slowing down of the heat dynamics with increasing solute concentration. Knowing the dynamics of the heat signal and its spectral response - of which the shape is given by the transient spectrum at long delays - we can correct the isotropic spectra of the OD stretch at all delay times for the heating contribution⁹⁷.

Figure 5.3 presents the isotropic transient absorption signals for water and the three studied sugars, after correcting for the heating contribution. All isotropic spectra show a strong bleaching signal around 2500 cm^{-1} due to the bleaching of the fundamental $v = 0 \rightarrow 1$ transition (ground-state bleaching and stimulated emission) and an induced absorption at frequencies below 2420 cm^{-1}

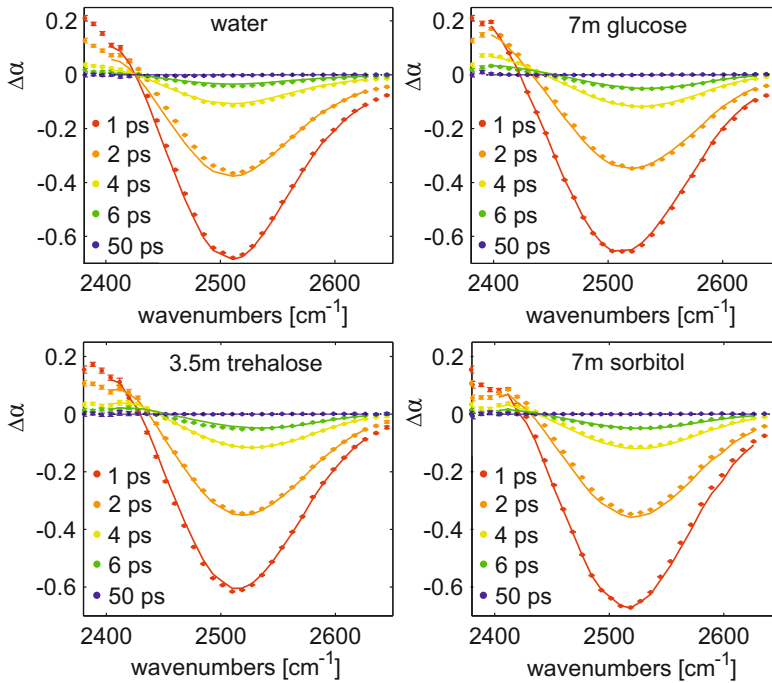


FIGURE 5.3. Isotropic absorption signals for solutions of glucose, trehalose and sorbitol in isotopically diluted water, at five different picosecond delay times after the excitation. The concentrations are given in molal (mol/kg). The solid lines represent fits using the model described in the text.

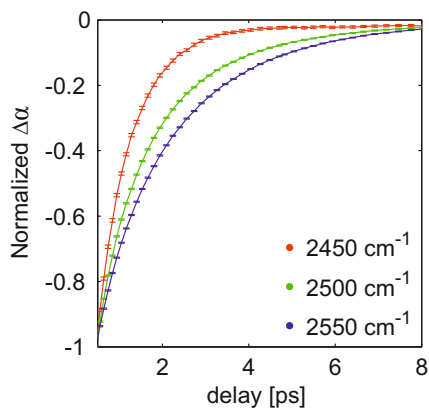


FIGURE 5.4. Isotropic absorption signal for a solution of 3.5 molal trehalose in water, shown for different probe frequencies as a function of delay time (normalized at 0.5 picoseconds).

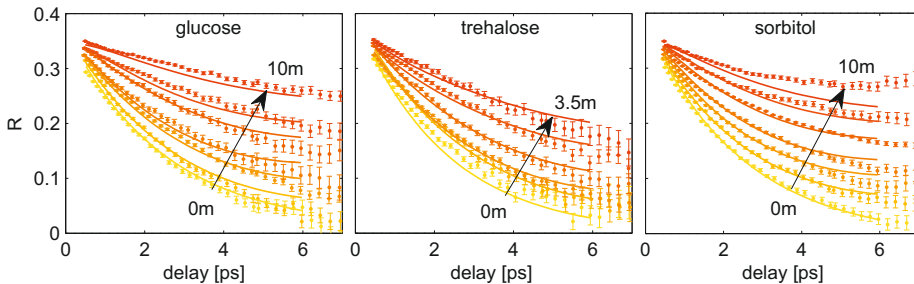


FIGURE 5.5. Anisotropic absorption signal at 2500 cm^{-1} for solutions of glucose, trehalose and sorbitol in water of different concentrations (trehalose: 0, 0.5, 1, 1.5, 2.5 and 3.5 molal). Solid lines are description with our model fit.

due to $\nu = 1 \rightarrow 2$ excited-state absorption. The spectral shapes are very similar for the different carbohydrates, even at high concentrations, in accordance with the linear spectra. For neat water, we find that the transient absorption signal decays with a frequency-independent time constant of 1.7 picoseconds, in agreement with earlier reports⁷⁴. This time constant represents the vibrational lifetime of the OD stretch vibration of HDO dissolved in H_2O .

The vibrational decay becomes quite inhomogeneous upon the addition of sugar: on the red side of the OD absorption band the decay speeds up compared to neat water, while on the blue side of the OD absorption band the decay slows down in comparison with neat water. This observation is further illustrated in figure 5.4, which shows the isotropic absorption change measured for a solution of 3.5 molal trehalose as a function of delay time at different probe frequencies. The inhomogeneity of the relaxation increases with increasing sugar concentration. This inhomogeneity follows from the fact that both water and sugar contain hydroxyl groups that contribute to the transient spectral response. The frequency-dependent decay of the isotropic spectra shows that the spectral responses and lifetimes of the water and sugar hydroxyl groups differ.

Figure 5.5 presents the anisotropy of the vibrational excitation (as defined by eq. 2.46) measured at 2500 cm^{-1} for the three sugars at different concentrations. With increasing concentration of sugar, the decay of the anisotropy strongly slows down. This is the case for glucose, trehalose and sorbitol. For neat water the anisotropy decays with a timescale of 2.5 ps, in agreement with earlier reports⁷⁴.

5.3.3 REFERENCE MEASUREMENTS IN DMSO

The transient absorption signals as shown in figure 5.3, 5.4 and 5.5 contain contributions from both water and sugar hydroxyl groups. To extract the water reorientation dynamics, we need to separate these contributions. To this purpose we performed reference measurements on solutions of the studied sugars in dimethylsulfoxide (DMSO). The carbohydrates will form similar hydrogen

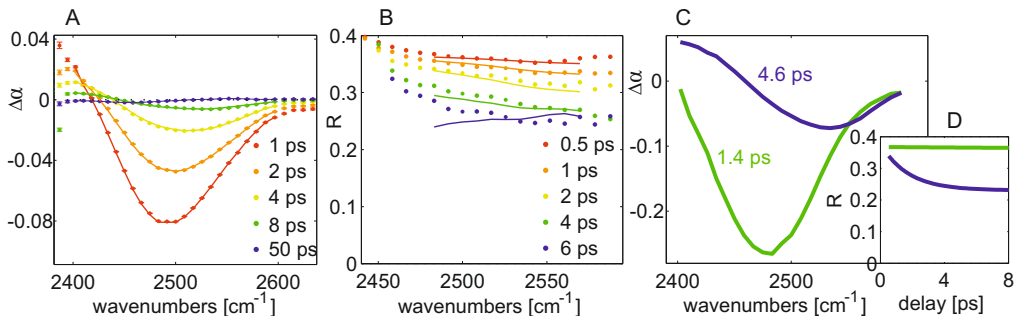


FIGURE 5.6. The isotropic absorption change (A) and the anisotropic absorption change (B) as a function of frequency for 0.4 molal 10% deuterated glucose in DMSO (solid lines are description with model fit). Spectral components (C) contributing to isotropic signal (relative amplitudes correspond to 1 ps), and anisotropy (D) of the two spectral components as a function of delay time.

bonds with DMSO as with water, but since DMSO itself does not contain hydroxyl groups, the transient absorption signals only represent the response from the OD stretch vibrations of the sugars. Figure 5.6 presents the isotropic and anisotropic signals of a solution of 0.4 molal glucose (10% deuterated) in DMSO. The decay of the isotropic absorption change is again observed to be frequency dependent: on the red side the decay is much faster than on the blue side of the OD absorption band. We find that the dynamics of the isotropic and anisotropic signals can be very well described with two spectral components, with vibrational relaxation time constants of 1.4 ± 0.2 picoseconds and 4.6 ± 0.2 picoseconds (figure 5.6C), and different associated anisotropy dynamics (figure 5.6D). The responses of trehalose and sorbitol dissolved in DMSO can also be very well described with two spectral components with different vibrational lifetimes and different associated anisotropy dynamics.

5.3.4 SPECTRAL DECOMPOSITION MODEL

Based on the findings for the sugar solutions in DMSO, we analyze the results measured for the sugar solutions in water with a model that includes two spectral components for the sugar response and one spectral component for the water response. In this model we assume that the relative amplitudes of the sugar and water components are only defined by the sugar concentration. We further assume that the spectral shape and lifetime of each component do not change with concentration, and fix the spectral shape and lifetime of the water component to the corresponding values for neat water (4% D₂O:H₂O). Each spectral component is assumed to show an associated anisotropy decay of the form:

$$R_i(t) = A_i e^{-t/\tau_i} + B_i \quad (5.1)$$

The anisotropy dynamics of the two sugar components are taken to be the same at all concentrations. Only the anisotropy decay of the water component is

allowed to vary with concentration. We fit this model to the isotropic absorption and anisotropy signals at all measured concentrations for each sugar. The fit is performed with a single fitting routine that adds the least-square errors for each concentration. During each iteration of the fit, the isotropic absorption signal is spectrally decomposed in three spectra $\sigma_i(\nu)$ for a given set of mono-exponentially decaying populations $N_i(t)$. The error is then determined by comparing the isotropic transient spectral response at all frequencies and delay times to the result of the spectral decomposition $\sum_i N_i(t)\sigma_i(\nu)$. The error for the anisotropic signal is determined by comparing each model anisotropy component R_j (given by A_j , B_j and τ_j) to the following quantity

$$\frac{\frac{1}{3}(\alpha_{\parallel} - \alpha_{\perp}) - \sum_{i \neq j} R_i N_i \sigma_i}{N_j \sigma_j} \quad (5.2)$$

Here α_{\parallel} and α_{\perp} are the measured parallel and perpendicular transient spectra, respectively. Equation (5.2) is based on the following expression, which follows from eqs. 2.41 and 2.46:

$$\frac{1}{3}(\alpha_{\parallel} - \alpha_{\perp}) = \sum_i R_i N_i \sigma_i \quad (5.3)$$

The result of the fits is displayed with solid lines in figure 5.3 and 5.5. The fits are in good agreement with the data for all sugars. The spectral components resulting from the fits are shown in the top row of figure 5.7. For all three sugars, the two components originating from the sugar hydroxyl groups are red-shifted and blue-shifted with respect to the water band, and have lifetimes around 0.4 ps and 3.8 ps respectively. The spectral shapes are very similar to what is found for the sugars in DMSO. For sorbitol the center frequencies of the two sugar hydroxyl bands are slightly closer together than for glucose and trehalose.

The anisotropy dynamics of the three spectral components are shown in the bottom row of figure 5.7. It is seen that the anisotropy of the two sugar hydroxyl components decays very slowly. The anisotropy dynamics of the water hydroxyl band are faster, but strongly slow down with increasing sugar concentration. We find that the final value of the anisotropy (coefficient B in eq. 5.1) of the water component stays within ± 0.015 for all sugars at all concentrations. Hence, the anisotropy decay of the water component can be well characterized by a single reorientation time constant τ_w of which the value depends on the nature of the sugar and its concentration. This reorientation time constant is presented in figure 5.8 for each sugar as a function of concentration.

5.3.5 MODELING WATER REORIENTATION OF SUGAR HYDRATION SHELLS

We measure the reorientation dynamics of water in sugar solutions up to very high concentrations. At the highest concentrations, only 5 to 6 water molecules (and 15 in the case of trehalose) are available per sugar molecule. As a result, the hydration shells of the sugar molecules will overlap, which implies

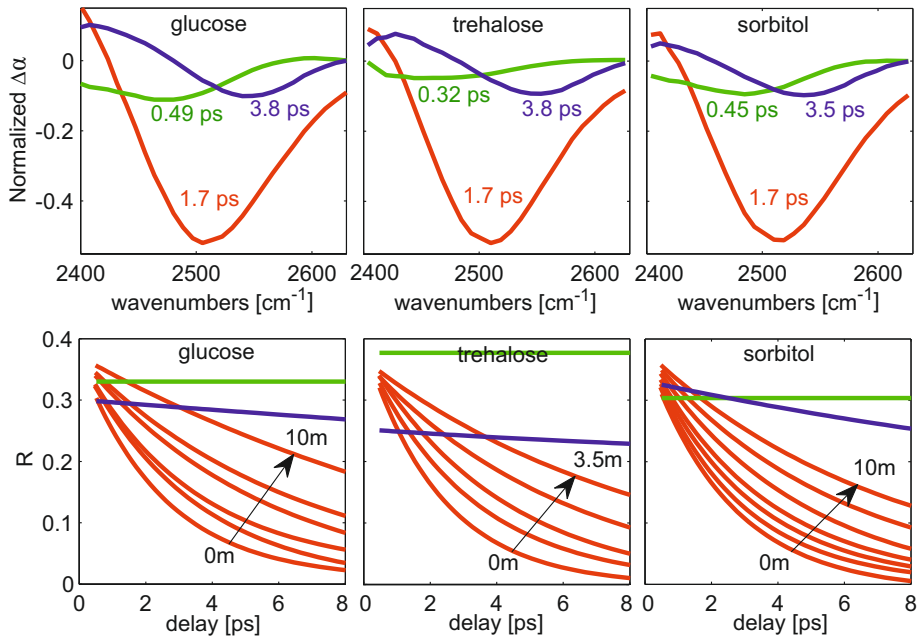


FIGURE 5.7. Top: Spectral components of the transient spectral response of aqueous sugar solutions. The spectral components decay with different vibrational lifetimes (indicated as legends). The three panels present the amplitudes of the spectral components at 1 ps after the excitation for the same sugar concentrations that are shown in figure 5.3). Bottom: Anisotropy as a function of delay time for the two sugar hydroxyl bands (green and blue) and the water hydroxyl band (red), at different sugar concentrations.

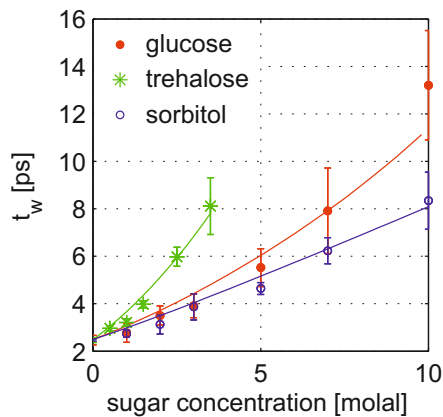


FIGURE 5.8. Water reorientation time constant as a function of sugar concentration. Solid lines represent the description with overlapping hydration shell model described in the text.

that the reorientation dynamics of the water molecules will be affected by the nearby presence of multiple sugar molecules. It is to be expected that the reorientation dynamics of water will become slower when the number of nearby sugar molecules increases. To account for this effect, we calculate the probabilities that a water molecule is located in zero, one, two or more sugar hydration shells. We assume the sugars to be randomly distributed, which is a reasonable assumption according to neutron diffraction experiments^{84,85} and MD simulations^{85,98}. The water molecules are largely randomly distributed as well, except for the fact that we do not allow a water molecule to belong to more than two hydration shells. The distribution depends on the sugar molar concentration C_M (calculated from the sugar molal concentration c_m with $C_M = c_m \cdot \rho / (1000 + c_m \cdot M_{sugar})$) and the size of the hydration shell, which is the number of water molecules dynamically perturbed by each carbohydrate. The calculation of the distribution of probabilities of the number of hydration shells to which a water molecule belongs is described in detail in the appendix of this chapter. To translate the distribution to the dynamics of water, we assign increasingly slow reorientation rates to water in zero, one, or two hydration shells. A single retardation factor x relates the reorientation rates, such that the rate decreases a factor x when going from zero to one hydration shell, and x^2 when going from one to two hydration shells. This model yields a triple exponential anisotropy decay R_{mdl} at each sugar concentration:

$$R_{mdl} = 0.4 \left(P_c(0)e^{-k_0 t} + P_c(1)e^{-k_0 x t} + P_c(2)e^{-k_0 x^2 t} \right) \quad (5.4)$$

where $P_c(i)$ is the probability that a water molecule belongs to i hydration shells, as calculated from the sugar concentration and the size of the hydration shell, and $k_0 = 1/2.5$ is the reorientation rate of unperturbed water. We can approximate eq. 5.4 well with a single time constant (in the interval of 0-8 picoseconds) to allow for a comparison with the time constant coming from the experiment at the same sugar concentration. Only two parameters, the retardation factor and the hydration shell size, are varied until the calculated water reorientation time constant is in accordance with the experimentally determined values, shown in figure 5.8. The calculated values are shown as solid lines in the same figure. We find an optimal retardation factor of 1.65 ± 0.15 , independently of the type of sugar, and hydration numbers of 24 ± 3 , 46 ± 5 and 22 ± 3 for glucose, trehalose and sorbitol, respectively.

5.4 DISCUSSION

5.4.1 SOLUTE DYNAMICS

For all investigated sugar solutions, the nonlinear vibrational response of the hydroxyl vibrations can be well described with three spectral components, each with its own vibrational relaxation time constant and associated anisotropy decay. The two components associated with the sugar hydroxyl groups probably do not represent two distinct species of sugar hydroxyl groups but rather

a continuous distribution of vibrational relaxation time constants across the inhomogeneously broadened sugar hydroxyl absorption band. The vibrational lifetime is observed to be significantly shorter in the red wing than in the blue wing of the absorption band. This is a quite general observation^{77,99,100} that follows from the fact that both the hydroxyl stretch frequency and the vibrational lifetime decrease with increasing strength of the hydrogen bond donated by the hydroxyl group. The shape and vibrational lifetime of the sugar hydroxyl components are very similar for glucose, trehalose and sorbitol. For sorbitol the two bands are slightly closer in frequency, which suggests that for sorbitol, the relaxation of the OD stretch vibrations is less inhomogeneous than for glucose and trehalose. This might be due to the lower chemical heterogeneity and the greater flexibility of the sorbitol molecule⁹⁸ compared to trehalose and glucose.

For all sugars, the anisotropy of the vibrational excitation of the hydroxyl stretch vibrations decays only partially within the experimental time window of ~ 10 ps. The partial decay indicates that the reorientation of the sugar hydroxyl groups occurs within a finite cone angle. The complete decay of the anisotropy requires the molecular reorientation of the entire sugar molecule, which takes tens of picoseconds^{90,92}. The sugar hydroxyl band at lower frequencies (green band in figure 5.7) has a higher and more persistent anisotropy value than the band at higher frequencies. This difference can be explained from the fact that the band at lower frequencies corresponds to more strongly hydrogen bonded hydroxyl groups for which the cone angle will be smaller. The anisotropy decay of the sugar components is not very different for sorbitol compared to glucose and trehalose, which indicates that the flexibility of the backbone of the sugar does not play a role for the hydroxyl reorientation dynamics occurring on a 10 ps time scale. The reorientation on this time scale is thus only governed by the strength of the local hydrogen-bond interaction.

5.4.2 WATER DYNAMICS

For all three sugars we observe a superlinear increase of the water reorientation time with sugar concentration. Based on our modeling of the water reorientation in the sugar hydration shells, we explain this superlinear behavior from a combination of two effects. The first is that the probability for a water molecule to belong to two or more hydration shells strongly increases with concentration. The second is that the reorientation of water molecules belonging to two or more hydration shells is slower than for water molecules belonging to a single hydration shell. In an NMR study of a solution of trehalose in water a similar superlinear increase of the reorientation time with concentration has been observed⁹⁰. This observation was interpreted as the result of water molecules interacting with multiple trehalose molecules, in agreement with our interpretation. A similar trend has been observed with dielectric relaxation (DR) measurements of solutions of glucose in water⁸⁹. In the NMR and the DR measurements the water dynamics are observed to slow down even more strongly with increasing concentration than in our measurements. A possible explanation may be that the NMR and DR results are more sensitive to col-

lective effects on the spin relaxation and the polarization response, whereas the femtosecond infrared experiments probe the reorientation of single hydroxyl groups.

We find that we can describe the increase in average water reorientation time with a model that assigns increasingly slow reorientation times to water molecules in zero, one or two carbohydrate hydration shells. From the model we extract a retardation factor of 1.65 ± 0.15 . This retardation factor implies that water molecules that are located within the hydration shell of one sugar molecule reorient 1.65 ± 0.15 times slower compared to water molecules in bulk water, while water molecules within the hydration shell of two sugar molecules reorient 2.7 ± 0.3 times slower again. Obviously, this discrete description of the water reorientation in the vicinity of sugars is an approximation of the actual, more diffuse, water reorientation, but it nonetheless indicates the magnitude and extent of the effect of sugars on the water dynamics in concentrated sugar solutions. Interestingly, the retardation is very similar for the different types of sugars. A similar observation was made using dynamic light scattering measurements⁹².

For all investigated sugars, the water reorientation in a solution with a particular sugar concentration can be described with a single reorientation time constant. This time constant increases strongly with increasing sugar concentration, reflecting an overall slowing down of the water reorientation. In contrast to the water dynamics around small amphiphilic molecules^{101,102} and salts^{77,99}, we do not observe a clear distinction between bulk-like water and hydration water. For these solutions, it was found that the reorientation of a fraction of the water molecules is strongly retarded, while the remaining water molecules were observed to reorient with the same time constant as observed for neat water, even at high solute concentrations. For the sugar solutions we do not observe such a bimodal distribution of the reorientation time of the water molecules. This finding indicates that the hydration layer in which the water dynamics are affected is far more diffuse around carbohydrates than around ions or hydrophobic molecular groups. The effect on the dynamics of water thus appears to be longer ranged for sugars than for ions or hydrophobic molecular groups.

The long-range character of sugar molecules on the dynamics of water may find its origin in their large number of hydrophilic hydroxyl groups. These hydroxyl groups will form strong hydrogen bonds with nearby water molecules⁹⁴, and thus it has been proposed that the effect of sugars on the dynamics of water scales with the number of hydrogen bonds between the sugar and water⁸⁸, or alternatively, with the number of sugar hydroxyl groups⁹². Following this idea, we plotted the water reorientation time constant against the number of sugar hydroxyl groups in figure 5.9A. It is apparent from the figure that the water reorientation time constants we measure do not follow the suggested scaling behavior. Trehalose has a comparatively strong effect on the water dynamics per hydroxyl group, while the effect of sorbitol is relatively weak. This is most apparent at sugar concentrations above 1 molal (trehalose) and 2 molal (glucose, sorbitol).

At higher concentrations, the effect of the overlapping hydration shells be-

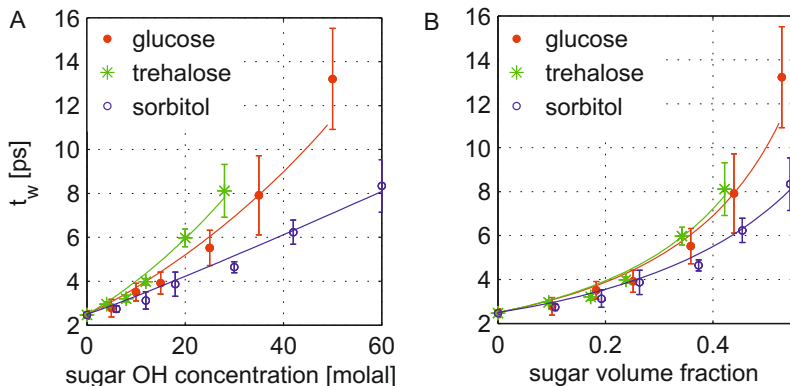


FIGURE 5.9. Water reorientation time constant as a function of (A) concentration of sugar hydroxyl groups and (B) sugar volume fraction.

comes important. In this regime the water dynamics are not only influenced by the hydrogen-bond interactions between the sugar molecules and water, but also by the volume that is left for water in between the sugar solutes. In this limit the volume occupied by the sugar solutes starts to play a role. The molecular weight and volume taken by trehalose are almost 2 times as large as for glucose. If we plot the water reorientation time against the sugar volume fraction, as determined from density measurements (figure 5.9B), we find that the water reorientation time constants in solutions of glucose and trehalose follow almost the same trend up to the highest concentrations.

For sorbitol the effect on the water dynamics is lower than for glucose and trehalose. In modeling the effect of sorbitol on the reorientation, we found that the hydration shell of sorbitol is somewhat smaller than for glucose, in spite of the fact that the molecular masses are nearly the same and sorbitol has 6 hydroxyl groups instead of 5. However, the molecular structure of sorbitol strongly differs from that of glucose and trehalose. The linear flexible structure of sorbitol allows for the formation of intramolecular hydrogen bonds⁹⁸, thus reducing the effect on the surrounding water molecules. The less strong effect of sorbitol on the water reorientation dynamics compared to glucose and trehalose thus likely finds its origin in their difference in molecular structure. For sugar molecules of similar structure like glucose and trehalose, the effect appears to scale quite well with the molecular volume, and surprisingly, less well with the number of hydroxyl groups. These findings suggest that the influence of sugars on the dynamics of the surrounding water involves collective structural effects in which the shape and size of the sugar molecule play important roles.

The long-range effects of sugars on the dynamics of water may in turn play a role in their influence on the conformation of proteins. Experiments show that trehalose is the most effective in preserving biomolecules, compared to other sugars, and most notably for concentrations above 1 M.⁸⁰ This is the concentration range for which we observe a larger effect of trehalose on the water

dynamics compared to glucose and sorbitol. The present results are therefore in line with an indirect protection mechanism of sugars via the water solvent.

5.5 CONCLUSIONS

We have investigated the molecular reorientation dynamics of water molecules in aqueous solutions of glucose, trehalose and sorbitol. With increasing sugar concentration, the decay of the OD stretch vibration becomes more inhomogeneous, due to an increasing contribution of sugar hydroxyl groups. We separate the contributions of sugar and water hydroxyl groups to the nonlinear vibrational signals using a spectral decomposition model. This allows us to observe the dynamics of water and sugar separately.

We find that the sugar hydroxyl groups only move in a restricted cone angle on the timescale of our experiment. The water reorientation is faster, but strongly slows down with increasing sugar concentration. Interestingly, the water reorientation can be characterized with a single reorientation time constant. We find that the water reorientation time τ_w increases from 2.5 ± 0.3 to 13 ± 2 ps for a solution with a glucose concentration of 10 molal, to 8 ± 1 ps for a solution with a trehalose concentration of 3.5 molal, and to 8 ± 1 ps for a solution with a sorbitol concentration of 10 molal. The fact that we do not observe a bimodal distribution of the reorientation time of the water molecules, as for aqueous solutions of small amphiphiles and salts, indicates that the hydration layer of sugars is more diffuse and extends over a longer range.

For all three sugars, the water reorientation time increases superlinearly with sugar concentration. We explain this superlinear dependence with the effect of overlapping hydration shells, and describe the water reorientation time with a model that assigns increasingly slower reorientation times to water molecules in zero, one, two or three carbohydrate hydration shells. From the model, we find that for all three studied sugars the retardation factor is 1.65 ± 0.15 . From the model we also find that the hydration shells of glucose, trehalose and sorbitol comprise approximately 24 ± 3 , 46 ± 5 , and 21 ± 3 water molecules, respectively. A comparison of the effects of the different sugars, suggests that the influence of sugars on the dynamics of the surrounding water involves collective structural effects in which the shape and size of the sugar molecule play important roles.

5.6 APPENDIX: HYDRATION SHELL MODEL

To calculate the probabilities that water molecules belong to 1, 2, 3, or even more hydration shells of sugar molecules, we consider a system containing N_s solute molecules. For each solute molecule the fully filled solvation shell has a volume x (x does not include the volume of the solute) of the total volume, and thus the total volume of the solvation shells in case the shells would not overlap is equal to $N_s x$. The volume x is given by $x = N_h v_w$, where N_h is the number of water molecules in the hydration shell and v_w is the volume of a water molecule

($0.018/N_A$ liter, with N_A Avogadro's number). N_s is equal to N_A times C_M , the solute molar concentration.

To determine the probabilities that a water molecule belongs to a particular number of hydration shells we consider picking N_s times a volume x out of 1 liter of the solution and calculate the probability that a molecule is within at least one of the picked volumes x . We define $a^{(1)} = N_s x$. At every selection a molecule has a chance of x to be chosen, and a chance of $1 - x$ not to be chosen. The probability that a molecule is not chosen after choosing N_s times a volume fraction x is equal to $(1 - x)^{N_s} = (1 - x)^{a^{(1)}/x}$. We arrive at the following probabilities of molecules belonging to 0, 1, 2, 3 solvation shells:

$$\begin{aligned} P^{(1)}(0) &= (1 - x)^{N_s} = (1 - x)^{a^{(1)}/x} = e^{-a^{(1)}} & (5.5) \\ P^{(1)}(1) &= N_s x (1 - x)^{N_s - 1} = a^{(1)} e^{-a^{(1)}} \\ P^{(1)}(2) &= \frac{N_s(N_s - 1)}{2} x^2 (1 - x)^{N_s - 2} = \frac{[a^{(1)}]^2}{2} e^{-a^{(1)}} \\ P^{(1)}(3) &= \frac{N_s(N_s - 1)(N_s - 2)}{6} x^3 (1 - x)^{N_s - 3} = \frac{[a^{(1)}]^3}{6} e^{-a^{(1)}}, \end{aligned}$$

where we used that $x \ll 1$. In general:

$$P^{(j)}(i) = \frac{[a^{(j)}]^i}{i!} e^{-a^{(j)}}, \quad (5.6)$$

where we changed the superscript (1) for the more general superscript (j), indicating the number of the iteration. It should be noted that $a^{(j)} = \sum_{i=0}^{\infty} i P^{(j)}(i)$.

For geometric reasons, a water molecule can only belong to a maximum number of solvation shells, which we define as k . To account for this fact, we redistribute the probabilities of molecules belonging to more than k shells over molecules belonging to less than k shells. This redistribution is performed with a statistical approach, and will again yield non-zero probabilities of molecules belonging to more than k shells. However, the sum of these probabilities will be smaller than in the first calculation. The procedure is repeated until there are only probabilities of molecules belonging to k shells or less. We define an excess volume $a_{ex}^{(j)}$ of $a^{(j)}$ that is contained in molecules belonging to $k + 1$ and even more solvation shells. For $j = 1$ the excess volume $a_{ex}^{(1)}$ is given by:

$$a_{ex}^{(1)} = \sum_{i=k+1}^{\infty} (i - k) P^{(1)}(i), \quad (5.7)$$

where the term $(i - k)$ is introduced to account for the fact that a molecule belonging to $i > k$ shells has been chosen $i - k$ times too much. The excess volume $a_{ex}^{(j)}$ has to be redistributed over molecules that belong to less than k solvation shells. As we will calculate the final distribution with an iterative procedure, applying several subsequent calculations of the redistribution of excess volumes $a_{ex}^{(j)}$, we define the distribution $P_c^{(j)}(i)$ as the distribution that results after the j 'th iteration. Obviously $P_c^{(1)}(i) = P^{(1)}(i)$.

To calculate the probability distribution of the redistribution of $a_{ex}^{(j)}$ we account for the fact that only molecules belonging to less than k shells can be selected. Hence, we renormalize $a_{ex}^{(j)}$ to the volume from which molecules can be selected in the next $j + 1$ selection round:

$$a^{(j+1)} = \frac{a_{ex}^{(j)}}{\sum_{i=0}^{k-1} P_c^{(j)}(i)} \quad (5.8)$$

Substitution of $a^{(j+1)}$ in equation (5.6) yields the distribution function $P^{(j+1)}(i)$ of the excess volume $a_{ex}^{(j)}$. The division by $\sum_{i=0}^{k-1} P_c^{(j)}(i)$ accounts for the fact that the total volume from which molecules can be selected in the $(j + 1)$ 'th round corresponds to the volume of the molecules that have only been selected $k - 1$ or less times after the j 'th round. The volume taken by these molecules is smaller than the original volume by a factor $\sum_{i=0}^{k-1} P_c^{(j)}(i)$. This means that the probability that a particular molecule is selected from this volume is larger than in the case that the excess volume $a_{ex}^{(j)}$ could have been picked from all molecules. This larger selection probability is expressed in the fact that $a^{(j+1)} > a_{ex}^{(j)}$. The distribution function $P^{(j+1)}(i)$ is used to determine the corrections to the total probability function $P_c^{(j)}(i)$.

Selection of molecules that belong to $P_c^{(j)}(i)$ in the $(j + 1)$ 'th round will lead to a decrease of $P_c(i)$, i.e. of the fraction of molecules belonging to i solvation shells, irrespective of whether these molecules are chosen 1, 2 or more times. On the other hand, $P_c(i)$ will increase if a molecule belonging to $P_c^{(j)}(i-l)$ is selected l times. The probability of selecting a molecule l times from a particular $P_c^{(j)}(i)$ is given by $P^{(j+1)}(l)P_c^{(j)}(i)$. Hence, the redistribution leads to the following expression for the new, corrected fraction $P_c^{(j+1)}(i)$ of molecules belonging to i solvation shells:

$$P_c^{(j+1)}(i) = P_c^{(j)}(i) - P_c^{(j)}(i) \sum_{l=1}^{\infty} P^{(j+1)}(l) + \sum_{l=1}^i P_c^{(j)}(i-l) P^{(j+1)}(l), \quad i \leq k \quad (5.9)$$

In case molecules from $P_c^{(j)}(i)$ ($i < k$) are selected two or more times ($P^{(j+1)}(i \geq 2) \neq 0$), the redistribution also leads to a non-zero probability of molecules belonging to $i > k$ solvation shells. As the maximum number of solvation shells to which a molecule can belong is defined by k , the probability of belonging to $i > k$ solvation shells needs to be redistributed over $P_c(i)$ ($i < k$). This is done in the following manner. First the probability of molecules of belonging to $i > k$ solvation shells is added to $P_c^{(j+1)}(k)$:

$$P_c^{(j+1)}(k) = P_c^{(j+1)}(k) + \sum_{i=0}^{k-1} P_c^{(j)}(i) \sum_{l=k-i+1}^{\infty} P^{(j+1)}(l) \quad (5.10)$$

The excess selections $i > k$ define a new excess volume $a_{ex}^{(j+1)}$ with a magnitude

given by:

$$a_{ex}^{(j+1)} = \sum_{l=2}^{\infty} P^{(j+1)}(l) \sum_{i=k-l+1}^{k-1} (i-k+l) P_c^{(j)}(i) \quad (5.11)$$

The case of $a_{ex}^{(1)}$, as expressed in equation (5.7), applies to the case before any selection was made, i.e. to $P_c^0(0) = 1$ and $P_c^0(i > 0) = 0$. The value of $a_{ex}^{(j+1)}$ evaluated with equation (5.11) is used in equation (5.8) to transfer $a_{ex}^{(j+1)}$ and $P_c^{(j+1)}(i)$ to $a^{(j+2)}$. Next, equation (5.6) is used to calculate the normalized distribution function $P^{(j+2)}(i)$, and equation (5.9) to calculate $P_c^{(j+2)}(i)$. The calculation is repeated until the probability of molecules belonging to $i > k$ solvation shells has become negligibly small ($\sum_i P_c(i > k) \approx 0$) or until all molecules are at least k times selected, meaning that $\forall P_c(i < k) = 0$.